Supplementary information for:

Urban Pollution Impact Assessment in Six Lithuanian Cities With a Focus on Road Traffic Emissions - Integrated Framework for Environmental Health Studies

Simonas Kecorius[a,b,c], Leizel Madueño[d], Wolfram Birmili[e], Jakob Löndahl[f], Kristina Plauškaitė[a], Steigvilė Byčenkienė[a], Mario Lovrić[g,h], Valentino Petrić[h,i], Manuel Carranza-García[j], Manuel J. Jiménez-Navarro[j], María Martínez-Ballesteros[j], Magdalena Weiss[b,k], Otmar Schmid[k,l], Josef Cyrys[b], Annette Peters[b,m,n], and Gaudentas Kecorius[o]*

[a]*Center for Physical Sciences and Technology (FTMC), Vilnius, Lithuania*
[b]*Institute of Epidemiology, Helmholtz Zentrum München, Neuherberg, Germany*
[c]*Augsburg University, Augsburg, Germany*
[d]*Leibniz-Institute for Tropospheric Research, Leipzig, Germany*
[e]*German Environment Agency, Berlin, Germany*
[f]*Lund University, Lund, Sweden*
[g]*Institute for Anthropological Research, Zagreb, Croat*
[h]*Lisbon Council, Brussels, Belgium*
[i]*Ascalia d.o.o., Čakovec, Croatia*
[j]*Department of Computer Languages and Systems, University of Seville*
[k]*Institute of Lung Health and Immunity (LHI), Helmholtz Zentrum München, Neuherberg, Germany*
[l]*Comprehensive Pneumology Center (CPC-M), Member of the German Center for Lung Research (DZL), Munich, Germany*
[m]*Ludwig-Maximilians-University Munich, Munich, Germany*
[n]*Centre for Cardiovascular Research, Partner Site Munich Heart Alliance, Munich, Germany*
[o]*Private Researcher, Kupiškis, Lithuania*

* *Correspondence to:* Simonas Kecorius
Email: simonas.kecorius@helmholtz-munich.de

This PDF file includes:

Supplementary text
Figures S1 to S13
Tables T1 to T3
Legends for Movies 0
Legends for Datasets 0

Other supplementary materials for this manuscript include the following:

Movies 0
Datasets 0

Supplementary Information Text
An extreme gradient boosting (XGBoost) model

The XGBoost is a scalable and efficient machine learning algorithm based on gradient boosted decision trees. It builds an ensemble of decision trees sequentially, where each new tree is constructed to correct the residual errors of the previous ones. By leveraging both first- and second-order gradient information and incorporating regularization terms, XGBoost reduces over-fitting while enhancing predictive performance and computational speed. Its robustness to skewed data, high computational efficiency, and superior predictive accuracy make it an excellent choice for air quality modeling using complex spatial datasets.

The models were trained on 80% of the data while reserving 20% for testing. Hyperparameter tuning was performed using 5-fold cross-validation (CV), where parameters such as the number of estimators (the number of boosting rounds), maximum tree depth, and learning rate were optimized to maximize the R^2 metric. Shortly, In XGBoost, hyperparameters control learning dynamics and model complexity. The learning rate (LR) governs step size during training, with low values (≤ 0.1) ensuring stability and higher values (≥ 0.3) accelerating learning but risking overfitting. The maximum tree depth (MD) influences non-linearity, where shallow trees (MD ≤ 3) approximate linear models, while moderate depths (MD = 4–8) capture complex interactions. The number of estimators (NE) defines boosting iterations, with higher values (≥ 500) improving refinement but increasing computation time. Model non-linearity is primarily dictated by MD and LR, with MD ≤ 3, LR ≥ 0.2, and NE ≤ 100 yielding near-linear behavior, while MD ≥ 7, LR ≤ 0.05, and NE ≥ 500 indicate high non-linearity. Over-fitting in model prediction was controlled by choosing the models where the difference in R^2 between 5-fold CV and test set was less than 0.05.

Supplementary Information Figures

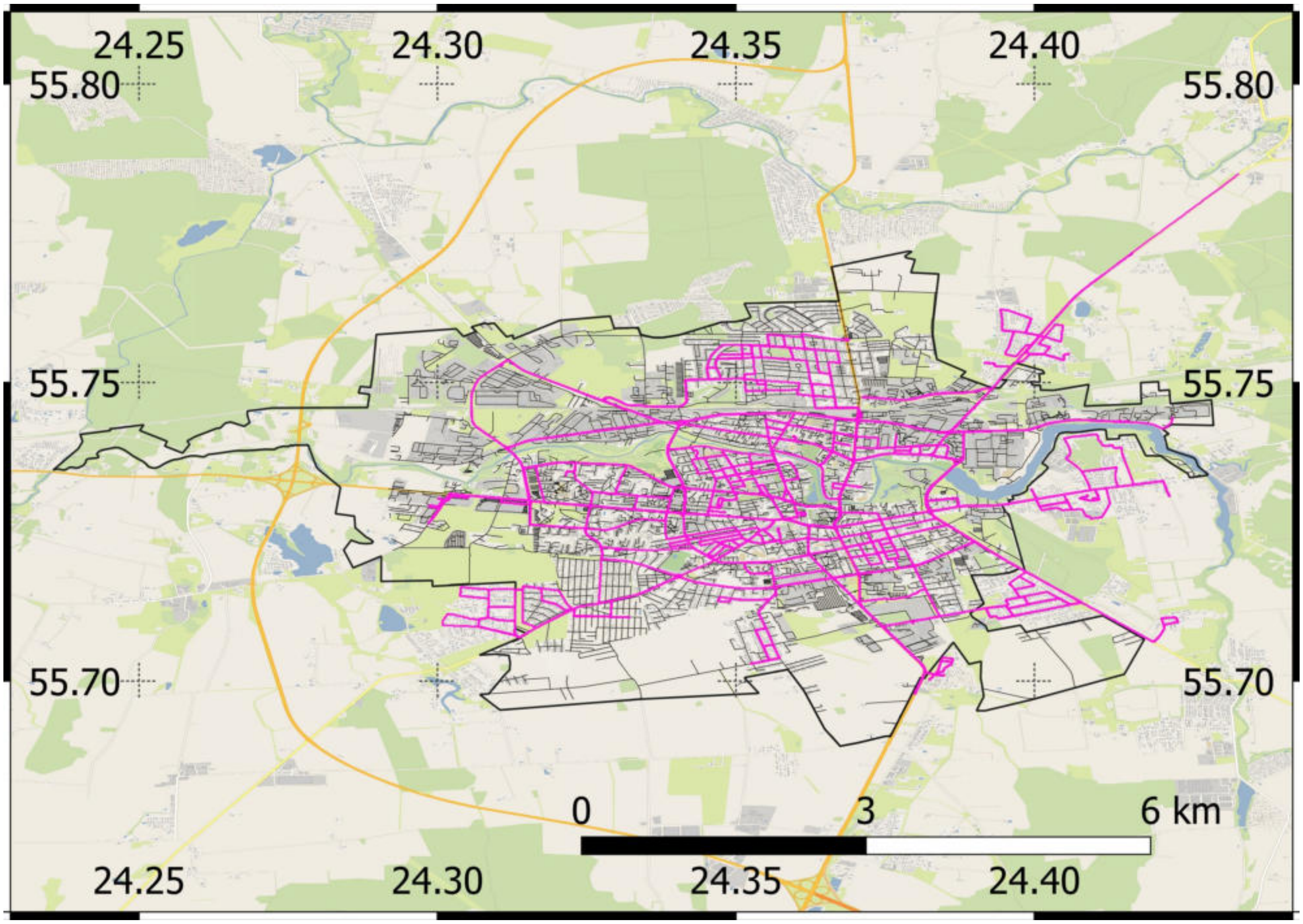

Fig. S1. Spatial extent of the measurements in Panevėžys. Grey contour line – city extent. Pink lines – measurement routes.

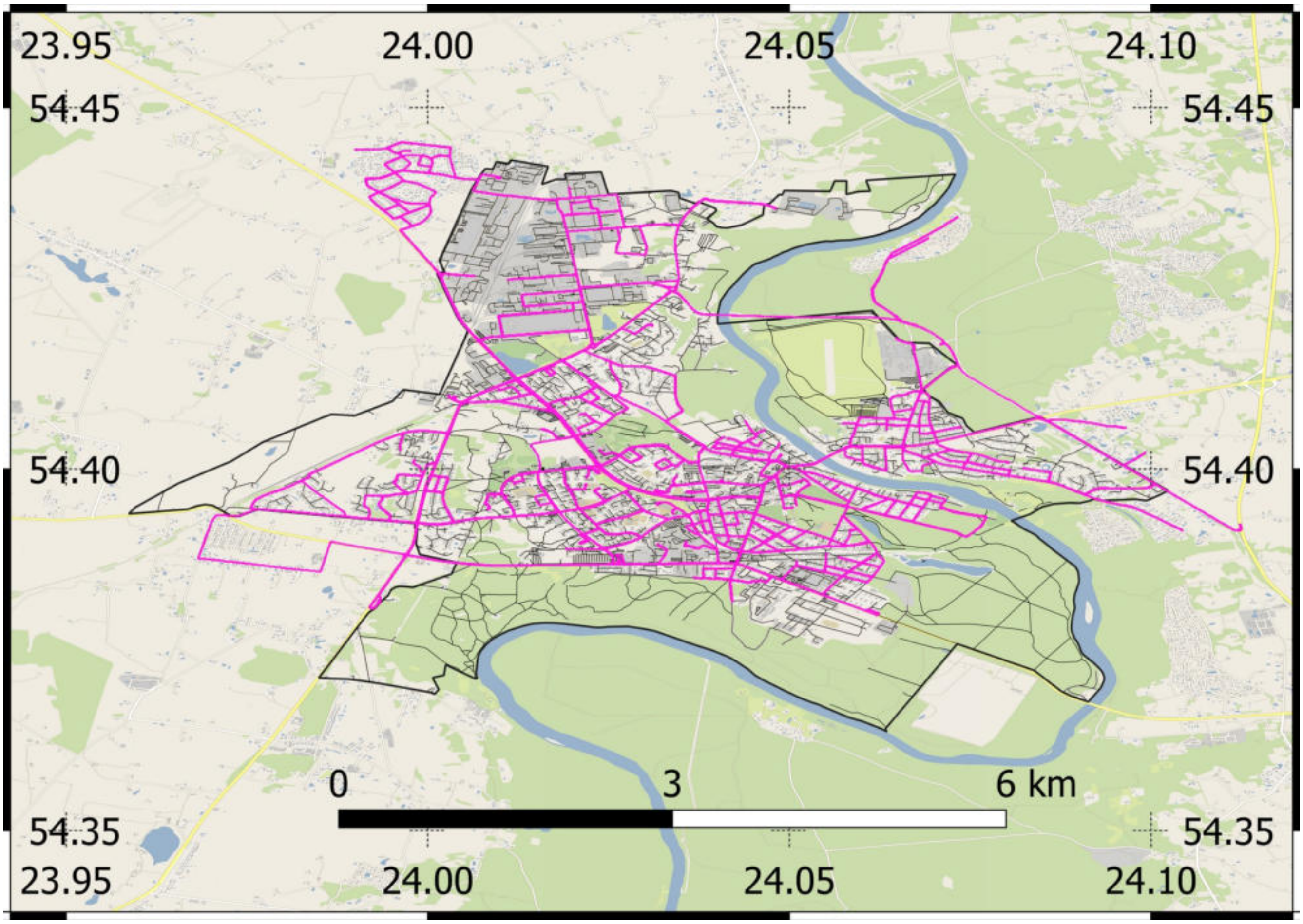

Fig. S2. Spatial extent of the measurements in Alytus. Grey contour line – city extent. Pink lines – measurement routes.

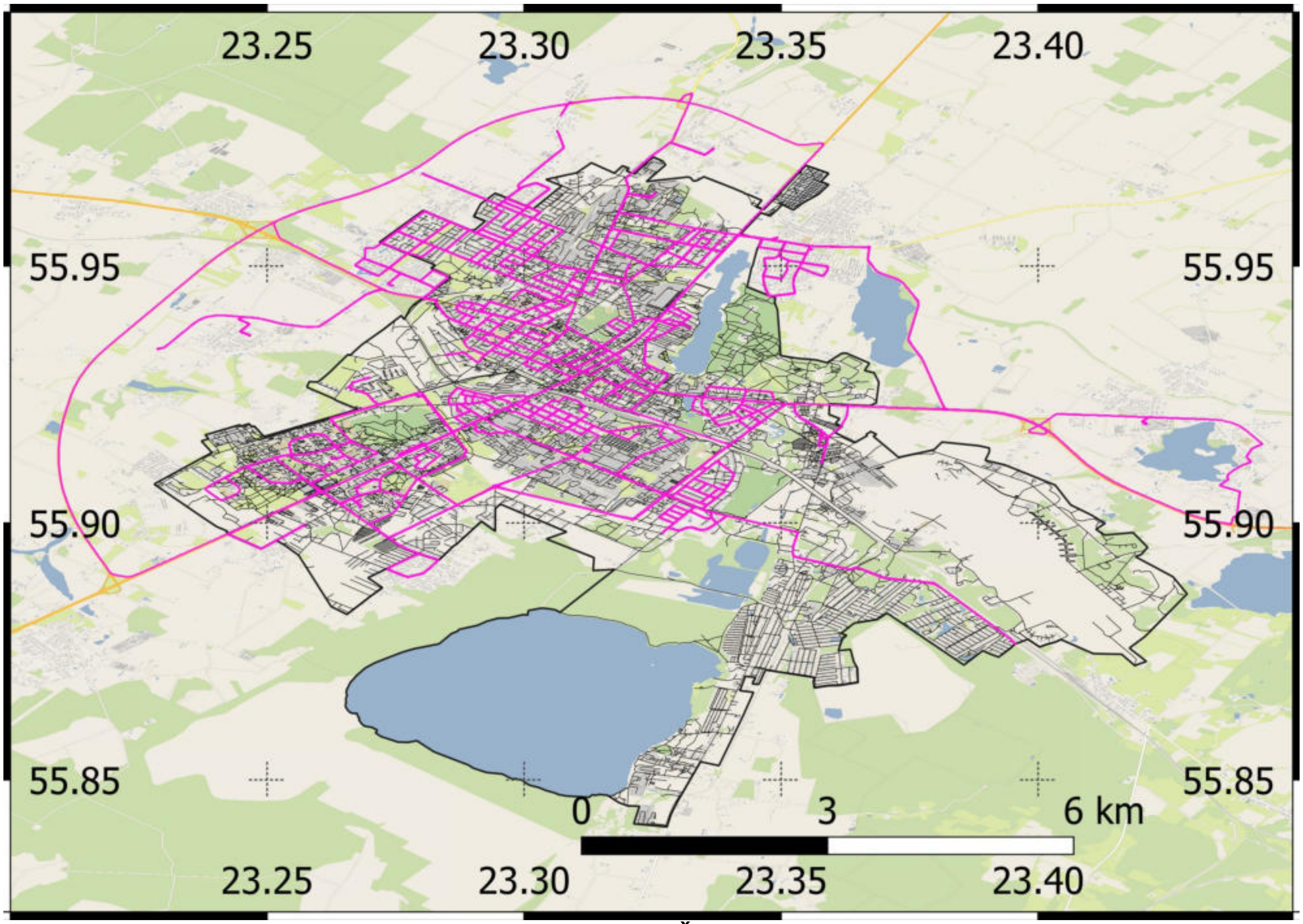

Fig. S3. Spatial extent of the measurements in Šiauliai. Grey contour line – city extent. Pink lines – measurement routes.

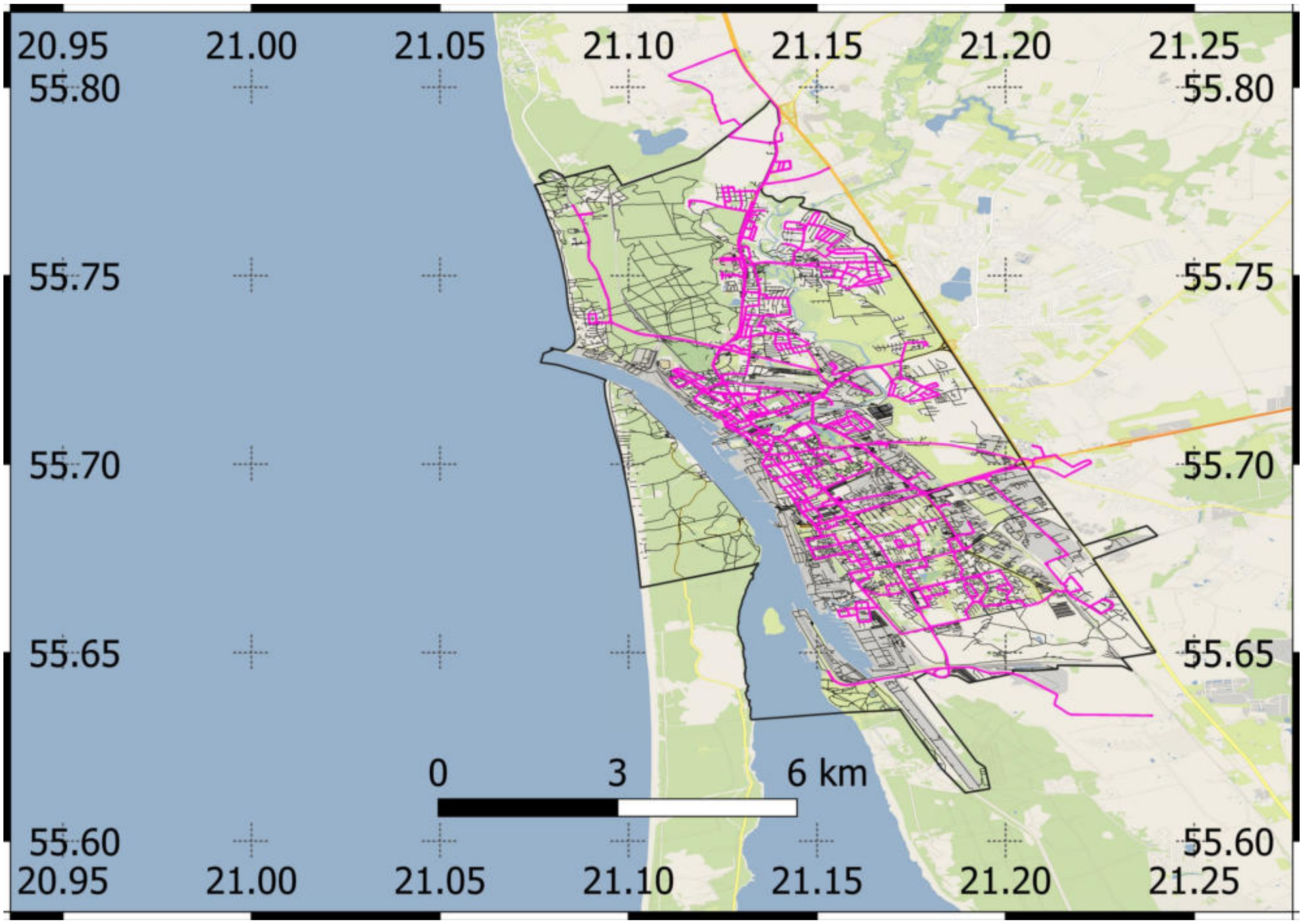

Fig. S4. Spatial extent of the measurements in Klaipėda. Grey contour line – city extent. Pink lines – measurement routes.

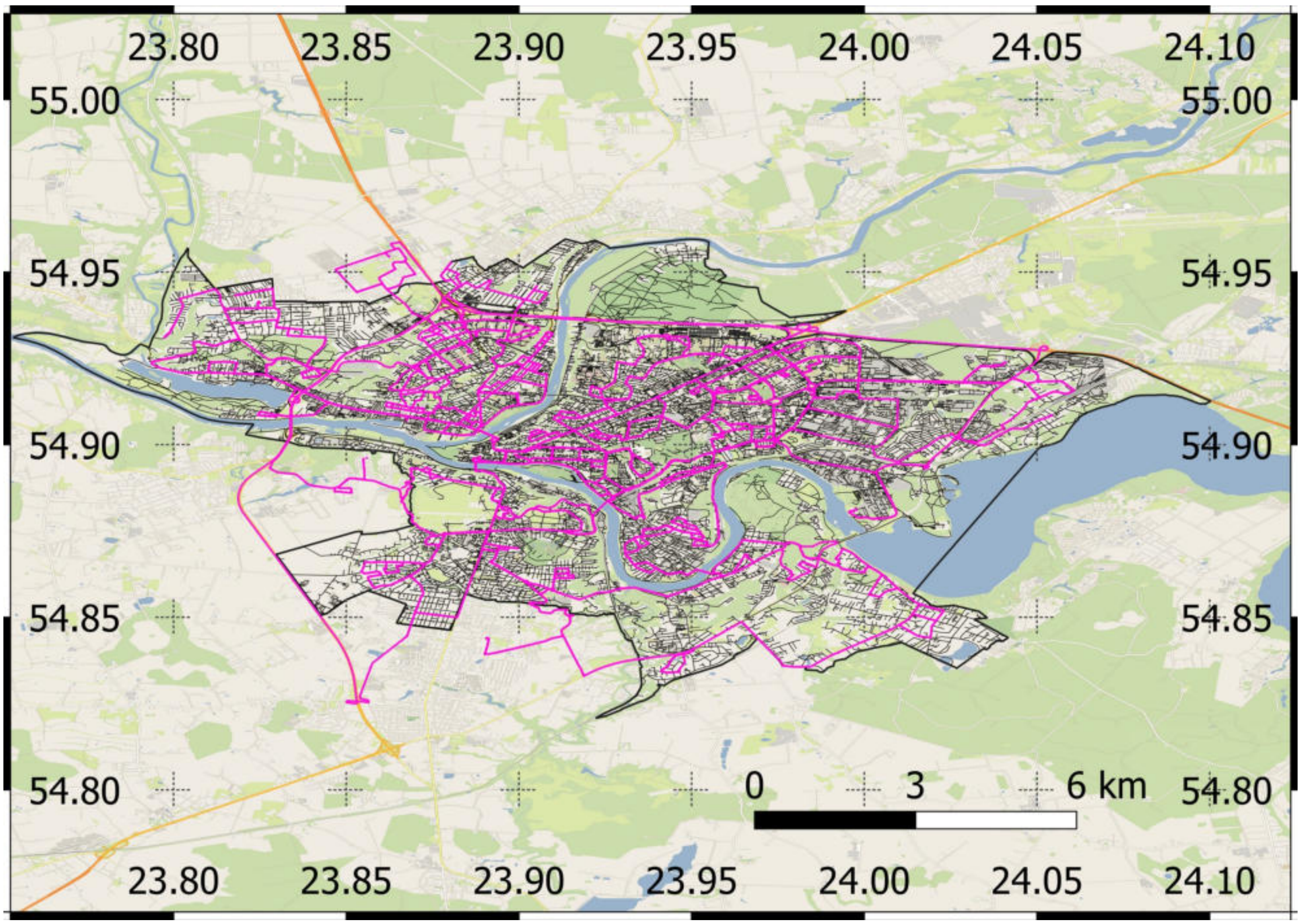

Fig. S5. Spatial extent of the measurements in Panevėžys. Grey contour line – city extent. Pink lines – measurement routes.

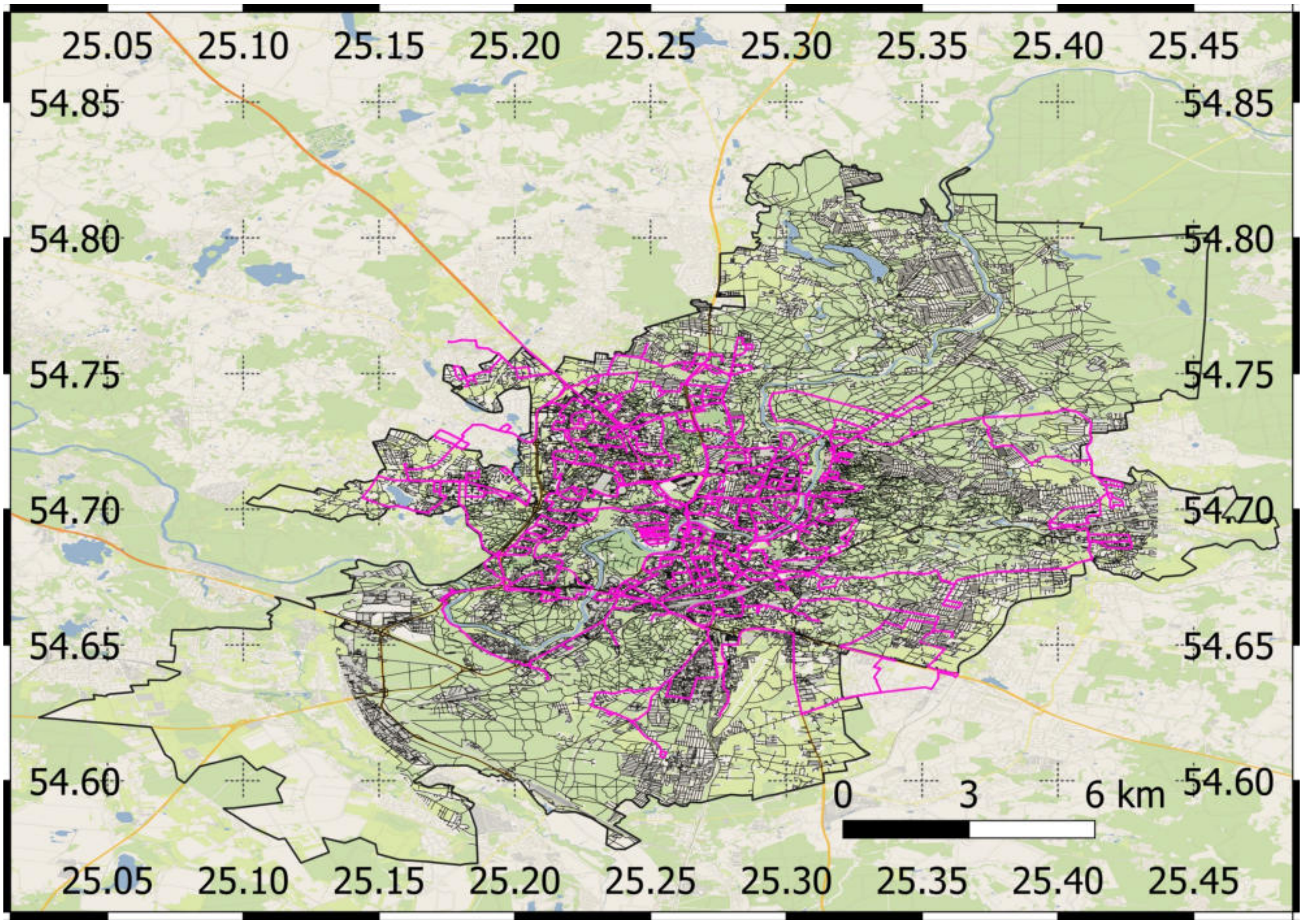

Fig. S6. Spatial extent of the measurements in Panevėžys. Grey contour line – city extent. Pink lines – measurement routes.

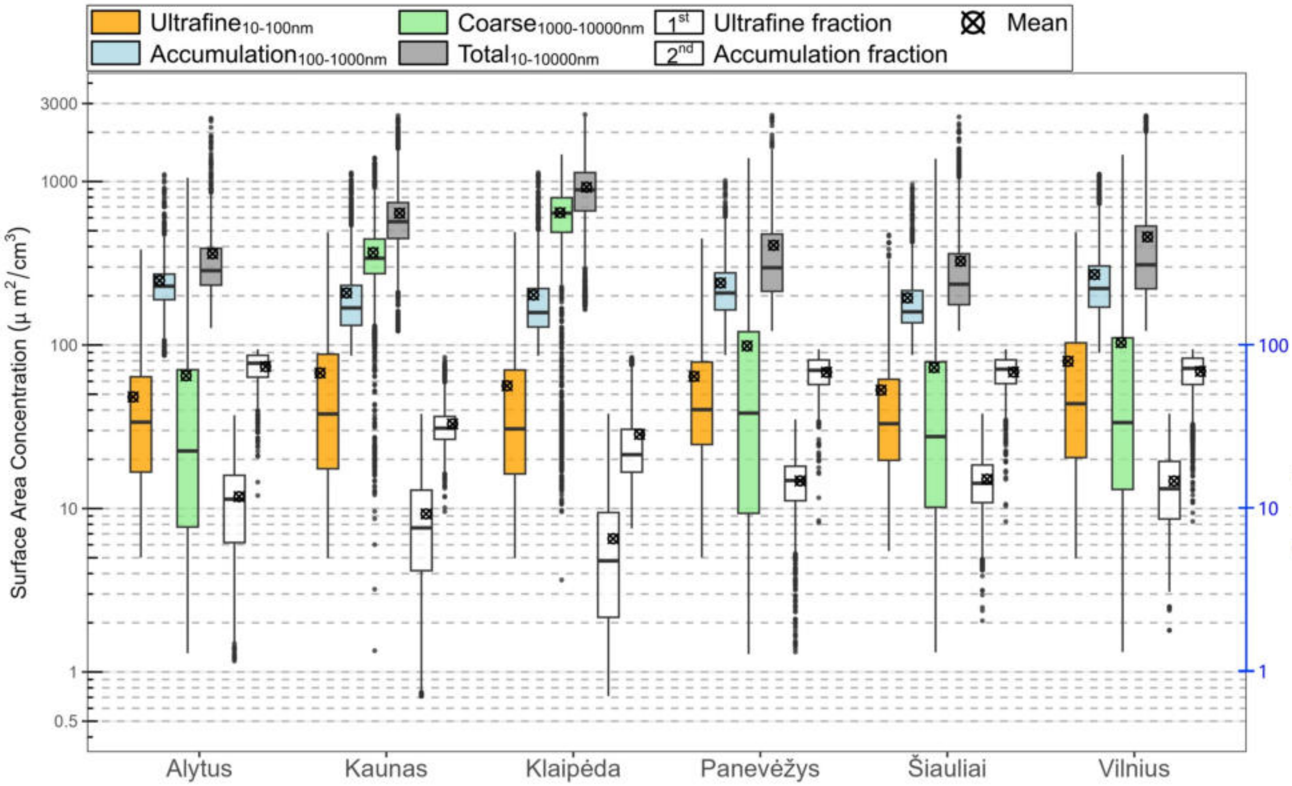

Fig. S7. The calculated surface area concentration in six Lithuanian cities. White bars represent ultrafine (first of two) and accumulation (second of two) mode surface area fractions (percentage of total surface area concentration).

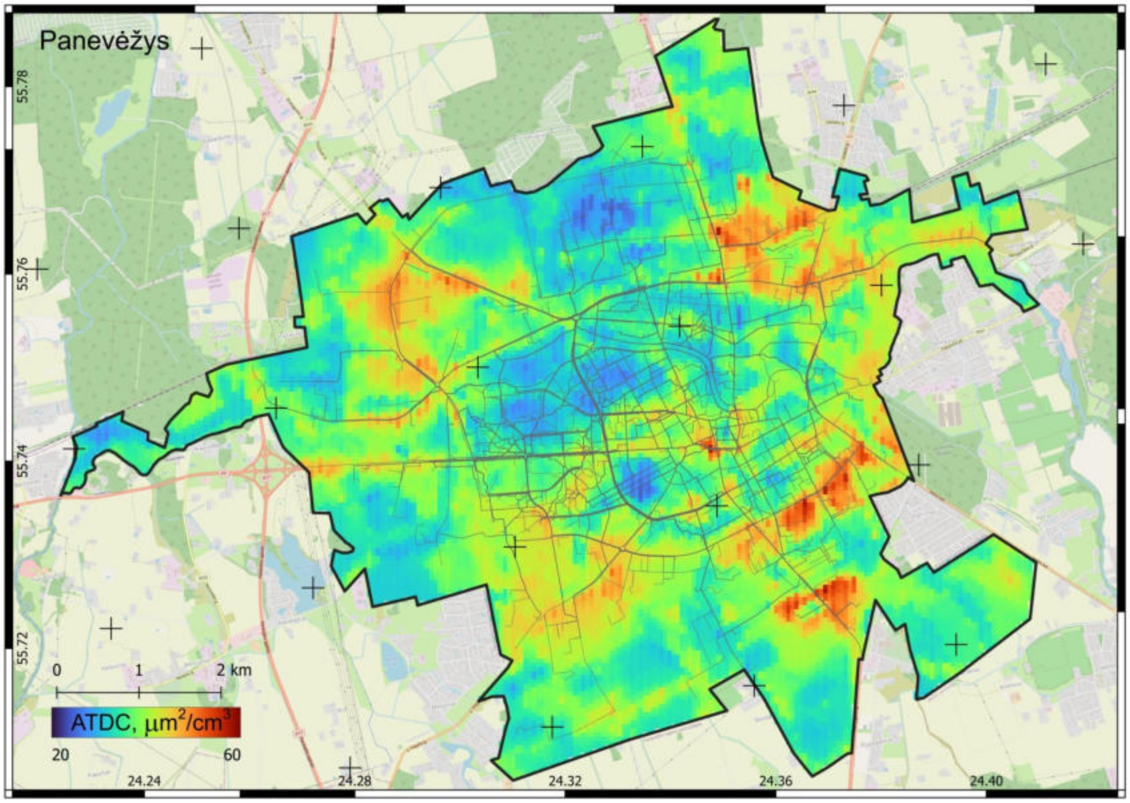

Fig. S8. Total alveolar deposited surface area concentration with synthesized roads for assessing the population proxy deposition dose while randomly walking in Panevėžys. Black contour line – city extent. Grey lines within the city – simulated routes.

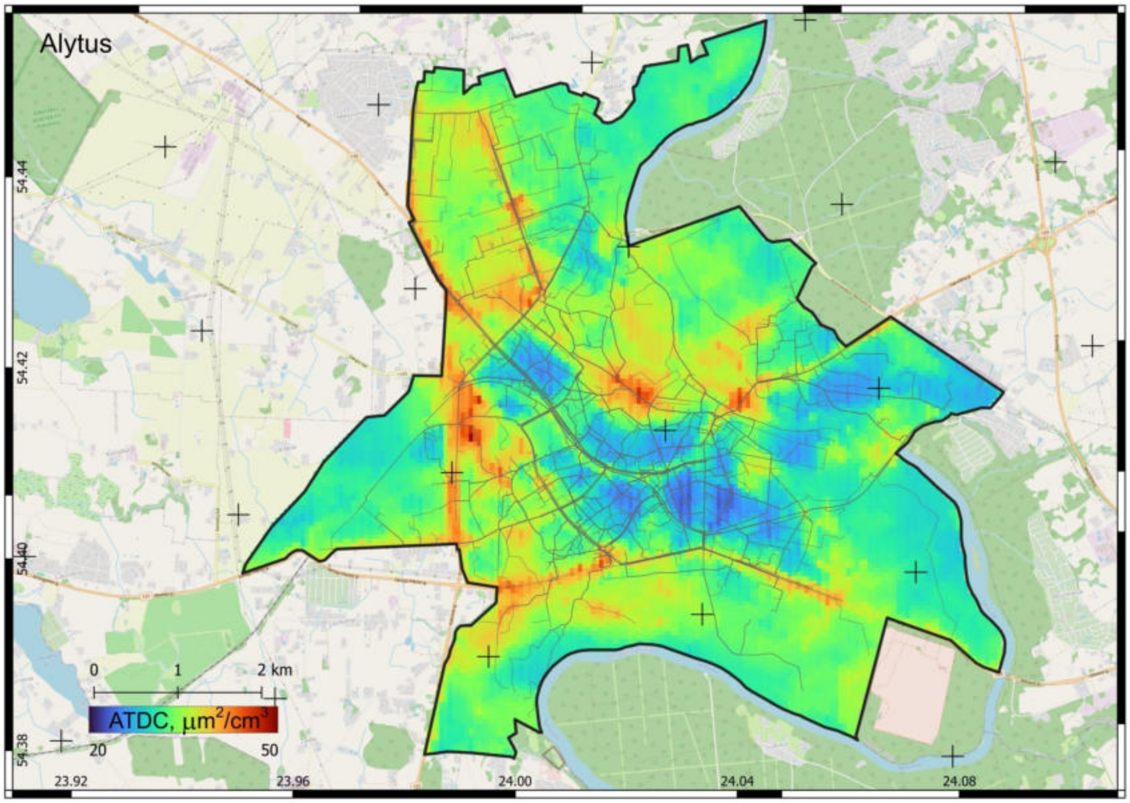

Fig. S9. Total alveolar deposited surface area concentration with synthesized roads for assessing the population proxy deposition dose while randomly walking in Alytus. Black contour line – city extent. Grey lines within the city – simulated routes.

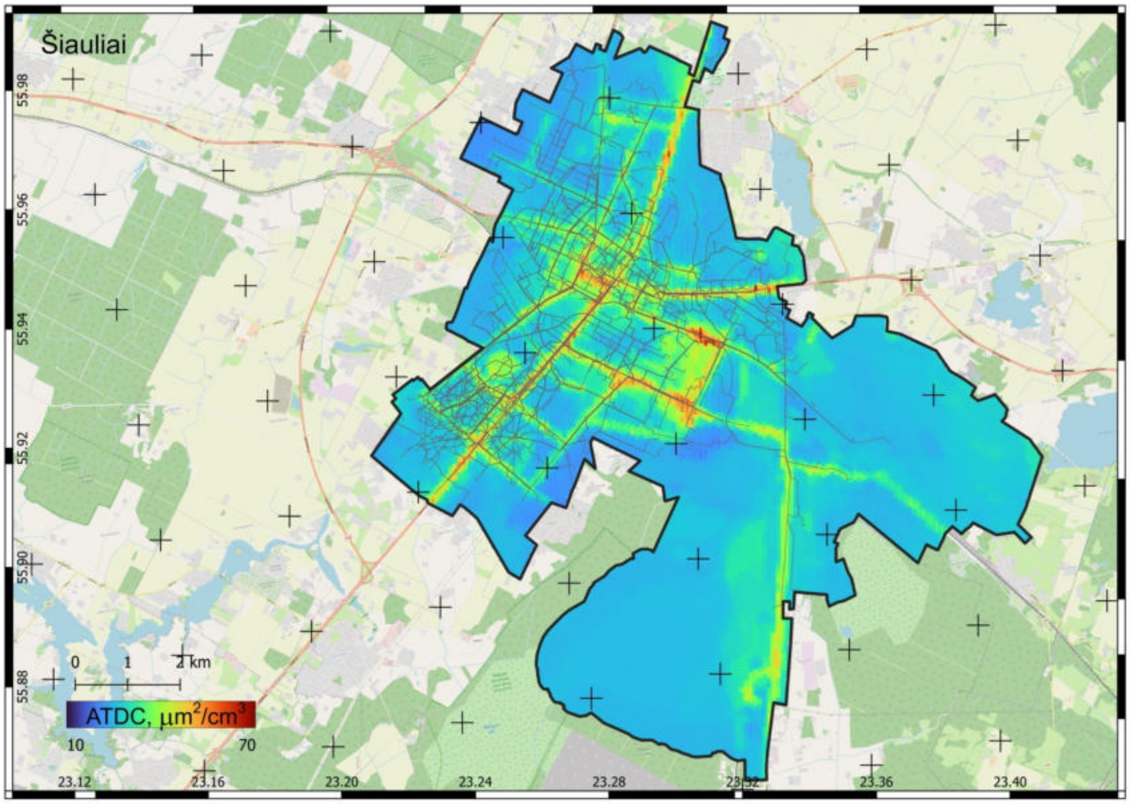

Fig. S10. Total alveolar deposited surface area concentration with synthesized roads for assessing the population proxy deposition dose while randomly walking in Šiauliai. Black contour line – city extent. Grey lines within the city – simulated routes.

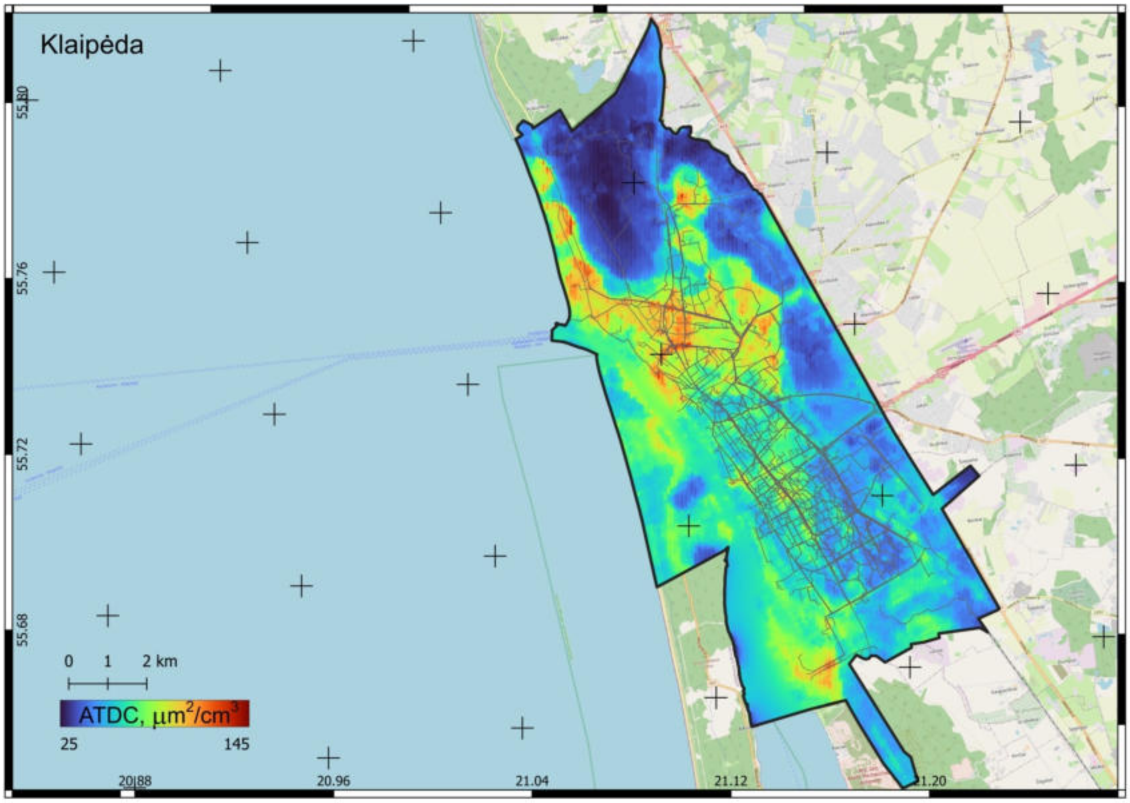

Fig. S11. Total alveolar deposited surface area concentration with synthesized roads for assessing the population proxy deposition dose while randomly walking in Klaipėda. Black contour line – city extent. Grey lines within the city – simulated routes.

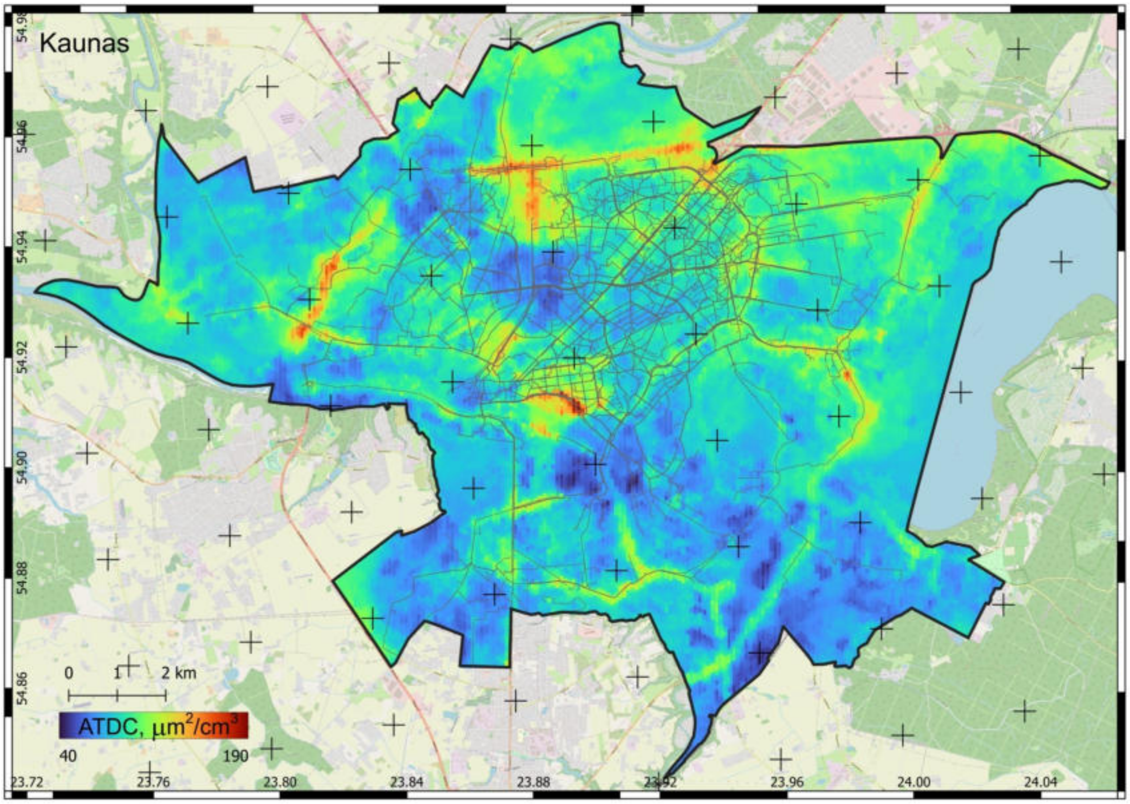

Fig. S12. Total alveolar deposited surface area concentration with synthesized roads for assessing the population proxy deposition dose while randomly walking in Kaunas. Black contour line – city extent. Grey lines within the city – simulated routes.

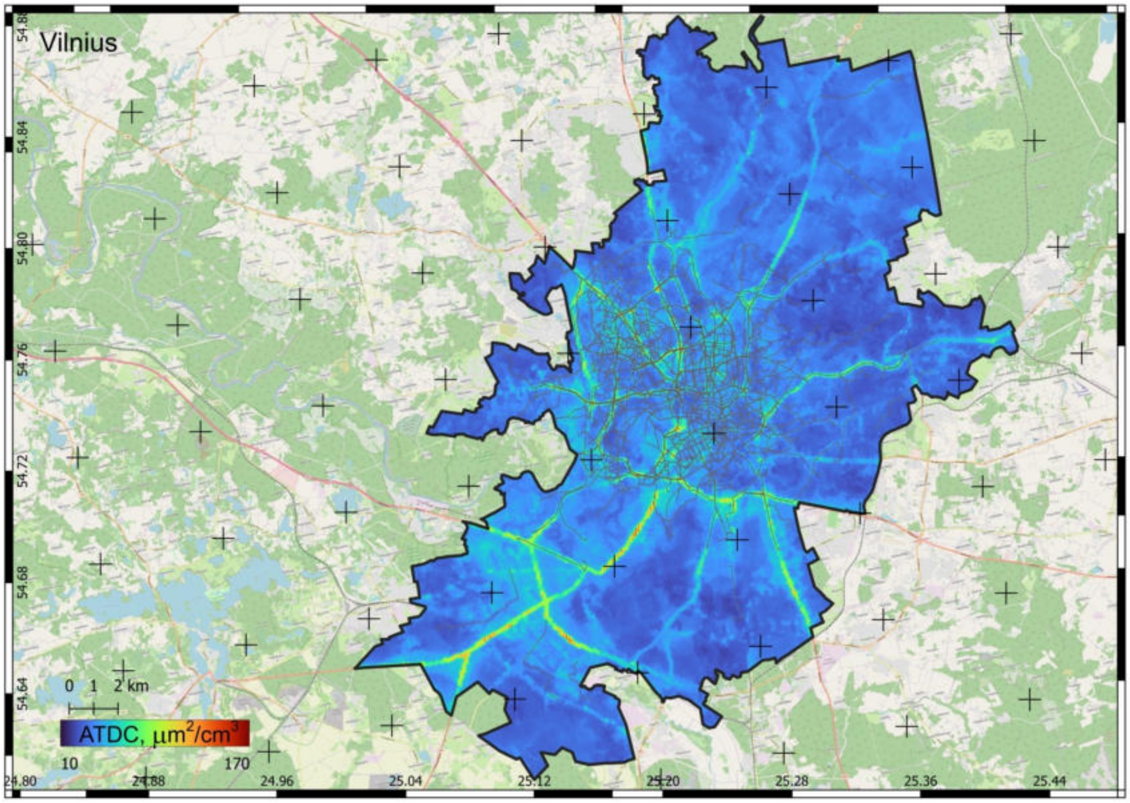

Fig. S13. Total alveolar deposited surface area concentration with synthesized roads for assessing the population proxy deposition dose while randomly walking in Vilnius. Black contour line – city extent. Grey lines within the city – simulated routes.

Supplementary Information Tables

Table T1. XGBoost model performance metrics for the best model with corresponding hyperparameter values. LR – learning rate, MD – max depth, NE – number of estimators. Please note that the information presented here correspond to only total alveolar deposited surface area concentration model.

City	Mode	5-fold CV mean R^2	Test set R^2	LR	MD
PNV	Ultrafine	0.5	0.5	0.01	6
	Accum.	0.43	0.47	0.05	6
	Total	0.54	0.57	0.05	6
ALY	Ultrafine	0.4	0.38	0.05	6
	Accum.	0.35	0.38	0.05	6
	Total	0.47	0.5	0.01	6
SIA	Ultrafine	0.51	0.56	0.05	8
	Accum.	0.49	0.5	0.01	6
	Total	0.44	0.47	0.01	6
KLA	Ultrafine	0.55	0.55	0.05	4
	Accum.	0.51	0.49	0.05	6
	Total	0.65	0.65	0.01	8
KAU	Ultrafine	0.58	0.59	0.05	4
	Accum.	0.56	0.61	0.05	8
	Total	0.61	0.65	0.05	6
VLN	Ultrafine	0.56	0.54	0.05	6
	Accum.	0.49	0.49	0.05	6
	Total	0.49	0.54	0.05	8

Table T2. Top 10 most important features presented as XGBoost gain metric (the average improvement in model performance, i.e., reduction in loss), which quantifies how valuable a feature is in reducing prediction error. The first letter and a word, separated by underscore, represents the feature class and feature sub-class, followed by buffer size. For example, R_Trunk100 represents cumulative trunk road length in 100 m buffer. The road and land use feature classes are encoded as R and L, respectively. Please note that the presented features correspond to only total alveolar deposited surface area concentration models.

Rank	PNV	ALY	SIA	KLA	KAU	VLN
1.	R_Trunk100	Noise1000	L_Heath1000	R_Second.Link1000	R_Bridleway1000	R_Trunk100
2.	R_Prim.Link1000	R_Primary100	R_Cycleway100	Building1000	R_Motorway100	R_Primary100
3.	R_Primary100	L_Commercial1000	R_Secondary100	R_Primary100	L_Commercia1000	Noise100
4.	R_Secondary100	Noise100	R_Trunk100	R_Trunk500	R_Trunk100	L_Heath500
5.	L_Cemetery1000	R_Tertiary1000	L_Cemetery1000	L_Commercial1000	Noise100	R_Secondary100
6.	R_Residential100	L_Meadow1000	R_Primary100	R_Track3Grade1000	L_Farm1000	R_Prim.Link1000
7.	L_Industrial1000	R_Tertiary100	R_Track3Grade1000	R_Track2Grade1000	R_Primary100	Noise1000
8.	R_Primary1000	L_Park1000	R_TrunkLink1000	L_Grass1000	R_Tertiary1000	R_LivingStreet1000
9.	R_Second.Link1000	R_Pimary500	L_Recreation500	L_Orchard1000	R_Prim.Link1000	R_Tertiary100
10.	R_Steps1000	L_Commercial100	R_MotorwayLink1000	L_Recreation1000	L_Nat.Reserve1000	Tertiary_R_1000

Table T3. Summary of street-level and background pollutant concentrations, as well as deposition doses for six Lithuanian cities.

Pollutant (meas. unit)	**Alytus**	**Kaunas**	**Klaipėda**	**Panevėžys**	**Šiauliai**	**Vilnius**
Street-level concentrations						
eBC_mean (ng/m^3)	2120	2612	2259	3171	2093	3237
eBC_sd (ng/m^3)	2807	3217	2914	3418	2818	3724
eBC_median (ng/m^3)	1133	1403	1164	2074	1035	1841
eBC_25th_pct. (ng/m^3)	666	634	542	1085	535	932
eBC_75th_pct. (ng/m^3)	2384	3279	2767	3808	2382	3945
PNC_mean (#/cm^3)	10041	13893	11216	14383	9965	15158
PNC_sd (#/cm^3)	12394	15954	13375	15933	12124	18497
PNC_N_median (#/cm^3)	6144	7533	6069	8584	5895	7841
PNC_25th_pct. (#/cm^3)	3804	3870	3359	5457	3818	3957
PNC_75th_pct. (#/cm^3)	10733	17292	13714	16446	10704	18443
UFP_mean (#/cm^3)	7947	11834	9218	11996	8178	12662
UFP_sd (#/cm^3)	11718	14618	11765	14686	11026	16854
UFP_median (#/cm^3)	4505	6075	4656	6754	4555	5927
UFP_25th_pct. (#/cm^3)	2181	2872	2456	3900	2800	2787
UFP_75th_pct. (#/cm^3)	8693	14626	11512	13547	8602	15058
ACCU_mean (#/cm^3)	2066	1882	1766	2246	1657	2286
ACCU_sd (#/cm^3)	1217	1604	1652	1476	1289	2091
ACCU_median (#/cm^3)	1693	1271	1197	1769	1227	1516
ACCU_25th_pct. (#/cm^3)	1495	937	829	1425	975	973
ACCU_75th_pct. (#/cm^3)	2150	2178	2018	2543	1751	2698
COARSE_mean (#/cm^3)	1.7	20.9	27.4	2.9	1.9	3.2
COARSE_sd (#/cm^3)	3.3	7.2	15.5	5	3.9	6
COARSE_median (#/cm^3)	0.6	20.6	27.5	1.1	0.6	1.2
COARSE_25th_pct. (#/cm^3)	0.2	16.5	20.7	0.4	0.2	0.6

COARSE_75th_pct. (#/cm^3)	1.8	24.8	34.9	3.3	1.9	3.2
ufp_nf_mean (%)	69.5	79.7	76.1	77.5	77.2	76.9
ufp_nf_sd (%)	14.2	9.1	11.3	10.6	8.9	10.5
ufp_nf_median (%)	71.3	79.9	77.3	78.3	77.2	76.8
ufp_nf_25th_pct. (%)	58.3	73.6	69.1	70.6	72.6	70.2
ufp_nf_75th_pct. (%)	80.1	86.2	84.3	85.6	82.8	84.5
accu_nf_mean (%)	25.5	20.6	22.9	22.5	22.9	23.3
accu_nf_sd (%)	9.3	8	9.1	9.2	7.7	8.9
accu_nf_median (%)	26.2	20.3	22	21.8	22.8	23.5
accu_nf_25th_pct. (%)	18.9	14.5	16	15.1	17.6	16.6
accu_nf_75th_pct. (%)	31.7	26	29.4	29	27.3	29.6
PSAC_mean ($\mu m^2/cm^3$)	361.6	639.5	922.8	407.3	325.9	458.5
PSAC_sd ($\mu m^2/cm^3$)	244.4	322.8	438.8	321.5	265.5	385.5
PSAC_median ($\mu m^2/cm^3$)	285.1	568	889.8	297	235.5	309.6
PSAC_25th_pct. ($\mu m^2/cm^3$)	232.3	448.2	661.3	213	176.5	220.7
PSAC_75th_pct. ($\mu m^2/cm^3$)	390.6	743.2	1134.2	476.9	361.7	534.3
UFP_SAC_mean ($\mu m^2/cm^3$)	48.2	67.5	56.3	64.3	53	79.5
UFP_SAC_sd ($\mu m^2/cm^3$)	47	75.4	66.6	63.9	56.6	88.9
UFP_SAC_median ($\mu m^2/cm^3$)	33.7	37.9	30.7	40.2	33	43.8
UFP_SAC_25th_pct. ($\mu m^2/cm^3$)	16.7	17.5	16.3	24.6	19.7	20.5
UFP_SAC_75th_pct. ($\mu m^2/cm^3$)	63.9	87.8	70.3	78.7	61.8	103.2
ACCU_SAC_mean ($\mu m^2/cm^3$)	247.7	208.3	202.5	239.5	194.1	270
ACCU_SAC_sd ($\mu m^2/cm^3$)	106.5	131.2	136.4	125.7	105.3	160.8
ACCU_SAC_median ($\mu m^2/cm^3$)	228.9	168.6	157.9	208.1	159.6	221.8
ACCU_SAC_25th_pct. ($\mu m^2/cm^3$)	189.4	131.8	128.9	163.9	136.8	170.5
ACCU_SAC_75th_pct. ($\mu m^2/cm^3$)	271.6	231.6	221.6	276.2	215.3	304.4
COARSE_SAC_mean ($\mu m^2/cm^3$)	64.8	367.4	644.7	98.8	72.8	103.4
COARSE_SAC_sd ($\mu m^2/cm^3$)	109.7	179.2	356.1	161.8	122.1	175.4

COARSE_SAC_median ($\mu m^2/cm^3$)	22.5	339.3	640.2	38.3	27.5	33.5
COARSE_SAC_25th_pct. ($\mu m^2/cm^3$)	7.7	273.3	489.2	9.4	10.2	13.1
COARSE_SAC_75th_pct. ($\mu m^2/cm^3$)	70.6	445	795.6	120.5	78.8	110.6
ufp_saf_mean (%)	11.8	9.3	6.5	14.8	15.1	14.7
ufp_saf_sd (%)	6.8	6.5	5.6	5.6	6	7.6
ufp_saf_median (%)	11.4	7.6	4.8	14.8	14.3	13.2
ufp_saf_25th_pct. (%)	6.2	4.2	2.2	11.2	10.9	8.6
ufp_saf_25th_pct. (%)	16	13	9.5	18.1	18.5	19.4
accu_saf_mean (%)	73.8	32.9	28.4	68.1	68.4	69
accu_saf_sd (%)	15.5	9.5	18.9	15.5	15.3	16.6
accu_saf_median (%)	77.4	31	21.4	70	71.1	72
accu_saf_25th_pct. (%)	63.6	26.5	16.7	57.3	58	57.4
accu_saf_75th_pct. (%)	86.5	36.6	30.5	81	81.1	83
TDSAC_mean ($\mu m^2/cm^3$)	126.4	341.2	568.3	159.9	124.9	180.9
TDSAC_sd ($\mu m^2/cm^3$)	124.7	181.1	291.1	168.2	133.9	199.3
TDSAC_median ($\mu m^2/cm^3$)	80.5	303.7	559.9	93.9	73.7	98.1
TDSAC_25th_pct. ($\mu m^2/cm^3$)	59.6	234.2	421.3	57.5	49.5	62.6
TDSAC_75th_pct. ($\mu m^2/cm^3$)	137.2	444.8	703.7	197.4	140.4	216
UFP_TDSAC_mean ($\mu m^2/cm^3$)	22.2	31.8	25.7	30.8	24.5	36.7
UFP_TDSAC_sd ($\mu m^2/cm^3$)	22.6	35.7	29.8	31.9	26.3	41.9
UFP_TDSAC_median ($\mu m^2/cm^3$)	15.3	17.7	14.2	19	15.3	19.8
UFP_TDSAC_25th_pct. ($\mu m^2/cm^3$)	7.2	8.1	7.4	11.9	9.2	9.2
UFP_TDSAC_75th_pct. ($\mu m^2/cm^3$)	27.9	41.5	32.5	37	28.2	47.2
ACCU_TDSAC_mean ($\mu m^2/cm^3$)	52.7	44.7	43.6	51.5	41.8	59.7
ACCU_TDSAC_sd ($\mu m^2/cm^3$)	24.7	30.1	31.4	28.6	24.4	37.6
ACCU_TDSAC_median ($\mu m^2/cm^3$)	47.5	34.6	33	43.8	33.5	48.2
ACCU_TDSAC_25th_pct. ($\mu m^2/cm^3$)	39.6	27.2	26.3	34.4	28.4	36.3
ACCU_TDSAC_75th_pct. ($\mu m^2/cm^3$)	57.9	50	48.3	58.6	46.2	67.3

COARSE_TDSAC_mean ($\mu m^2/cm^3$)	51.8	266.1	487.9	77.6	58.1	82.1
COARSE_TDSAC_sd ($\mu m^2/cm^3$)	87.1	145.3	269.3	125.4	97.4	138.3
COARSE_TDSAC_median ($\mu m^2/cm^3$)	18.1	239.7	483.5	30.3	21.9	26.7
COARSE_TDSAC_25th_pct. ($\mu m^2/cm^3$)	6.2	183.8	370.4	7	8.3	9.8
COARSE_TDSAC_75th_pct. ($\mu m^2/cm^3$)	56.9	332	606	96	62.9	89.2
ufp_dsaf_mean (%)	16.6	9	6.2	20.5	20.6	19.5
ufp_dsaf_sd (%)	8.6	7.2	6.7	7.4	7.4	9.1
ufp_dsaf_median (%)	16	7	3.6	20.3	19.9	17.6
ufp_dsaf_25th_pct. (%)	9.7	3.6	1.6	15.3	15.8	12.7
ufp_dsaf_75th_pct. (%)	21.7	12.3	8.3	25.4	24.9	24.5
accu_dsaf_mean (%)	53.9	14.3	13.1	46.1	45.8	48.2
accu_dsaf_sd (%)	20	7.1	14.5	18.8	17.7	19.8
accu_dsaf_median (%)	54.7	12.4	7.2	44.8	45.7	48.6
accu_dsaf_25th_pct. (%)	37.6	9.8	5.3	30.5	31.3	32.1
accu_dsaf_75th_pct. (%)	71	16.4	11.9	62.6	60.7	64.5
ADSAC_mean ($\mu m^2/cm^3$)	46.1	103.3	159.4	55.9	44.5	64
ADSAC_sd ($\mu m^2/cm^3$)	34.5	51.4	76.7	49.8	39.7	60.1
ADSAC_median ($\mu m^2/cm^3$)	34.2	93.4	158.3	36.9	29.6	40.5
ADSAC_25th_pct. ($\mu m^2/cm^3$)	27	71.8	115.7	26.4	21.7	25.9
ADSAC_75th_pct. ($\mu m^2/cm^3$)	50.8	129.5	199.5	65.9	49.8	78.1
UFP_ADSAC_mean ($\mu m^2/cm^3$)	13.1	18.8	15.4	18.2	14.5	21.7
UFP_ADSAC_sd ($\mu m^2/cm^3$)	13.3	21.2	18	18.8	15.6	24.7
UFP_ADSAC_median ($\mu m^2/cm^3$)	9	10.5	8.5	11.3	9.1	11.8
UFP_ADSAC_25th_pct. ($\mu m^2/cm^3$)	4.3	4.8	4.4	7	5.5	5.5
UFP_ADSAC_75th_pct. ($\mu m^2/cm^3$)	16.6	24.6	19.3	21.8	16.9	27.9
ACCU_ADSAC_mean ($\mu m^2/cm^3$)	25.6	22.1	21.5	25.8	20.4	28.7
ACCU_ADSAC_sd ($\mu m^2/cm^3$)	11.9	15.8	16.2	14.9	12.5	19.5
ACCU_ADSAC_median ($\mu m^2/cm^3$)	22.9	16.7	16	21.7	16.1	22.5

ACCU_ADSAC_25th_pct. ($\mu m^2/cm^3$)	19.3	13	12.5	17.1	13.6	16.6
ACCU_ADSAC_75th_pct. ($\mu m^2/cm^3$)	28.1	24.8	23.9	28.9	22.4	32.7
COARSE_ADSAC_mean ($\mu m^2/cm^3$)	7.2	63.2	115.7	11.5	8.7	12.7
COARSE_ADSAC_sd ($\mu m^2/cm^3$)	12.4	30.9	62.7	20.1	16.5	24.3
COARSE_ADSAC_median ($\mu m^2/cm^3$)	2.4	58.9	117.9	4.5	3.1	3.9
COARSE_ADSAC_25th_pct. ($\mu m^2/cm^3$)	0.8	45.9	88.8	1.2	1.2	1.6
COARSE_ADSAC_75th_pct. ($\mu m^2/cm^3$)	8	76.7	149.7	13.4	9.1	12.7
ufp_adsaf_mean (%)	24.5	16.3	11.4	30.2	31.1	29.5
ufp_adsaf_sd (%)	12.1	11.3	10.5	9.7	9.4	11.9
ufp_adsaf_median (%)	24.5	13.5	7.7	30.6	30.5	27.9
ufp_adsaf_25th_pct. (%)	14.2	7.2	3.3	24.2	24.8	19.9
ufp_adsaf_75th_pct. (%)	32.8	23.3	16.6	36.5	37.1	37.6
accu_adsaf_mean (%)	61.9	21.9	19.4	55.2	54.8	56.2
accu_adsaf_sd (%)	16.8	8.6	16.9	14.5	14.5	16.5
accu_adsaf_median (%)	62.6	19.8	12.4	54.8	55.5	56.8
accu_adsaf_25th_pct. (%)	50.3	16	9.2	45.4	44.9	44.2
accu_adsaf_75th_pct. (%)	74.9	25.5	20.7	65.5	65.5	70.1
Background concentrations						
eBC_mean (ng/m^3)	378	481	405	472	364	711
PNC_mean ($\#/cm^3$)	4187	3710	3022	5146	3774	3767
UFP_mean ($\#/cm^3$)	2686	2738	2097	3715	2770	2672
ACCU_mean ($\#/cm^3$)	1468	899	829	1355	963	1004
COARSE_mean ($\#/cm^3$)	0.1	18.5	27.9	0.1	0.1	0.3
PSAC_mean ($\mu m^2/cm^3$)	230.5	465.9	773.4	196.1	168	210.7
UFP_SAC ($\mu m^2/cm^3$)	21.3	16.4	13.7	22	19.4	19
ACCU_SAC ($\mu m^2/cm^3$)	203.7	131.8	128.5	166	140.1	179.1
COARSE_SAC ($\mu m^2/cm^3$)	0.8	290.2	609.1	0.6	1.1	1.5
TDSAC_mean ($\mu m^2/cm^3$)	54.5	255.3	502.8	48.7	43	53

UFP_TDSAC_mean ($\mu m^2/cm^3$)	9.4	7.6	6.3	10.1	9.1	8.6
ACCU_TDSAC_mean ($\mu m^2/cm^3$)	42	26.8	26.1	34.5	28.9	38.3
COARSE_TDSAC_mean ($\mu m^2/cm^3$)	0.5	204.7	457.6	0.4	0.8	0.7
Alveolar deposited surface area dose per 1 km commuting						
ADSAD_mean (mm^2 ± CV)	26.1 ± 50.9%	37.2 ± 27.0%	32.0 ± 35.9%	27.3 ± 47.4%	26.5 ± 49.1%	28.0 ± 44.4%
UFP_ADSAD_mean (mm^2 ± CV)	5.8 ± 54.7%	7.8 ± 37.4%	7.1 ± 39.1%	7.3 ± 37.1%	7.0 ± 42.3%	7.6 ± 37.8%
ACCU_ADSAD_mean (mm^2 ± CV)	11.9 ± 31.1%	10.8 ± 38.8%	10.6 ± 38.9%	10.7 ± 38.9%	10.7 ± 39.1%	12.1 ± 31.4%
COARSE_ADSAD_mean (mm^2 ± CV)	8.3 ± 96.7%	18.6 ± 32.5%	14.4 ± 50.1%	9.3 ± 85.6%	8.9 ± 89.1%	8.4 ± 89.8%
ufp_adsadf_mean (% ± CV)	22.2 ± 25.3%	21.0 ± 25.8%	22.4 ± 22.9%	29.0 ± 23.2%	28.2 ± 23.7%	28.4 ± 21.8%
accu_adsadf_mean (% ± CV)	52.9 ± 31.7%	28.9 ± 27.3%	33.7 ± 27.0%	42.0 ± 25.4%	43.8 ± 27.3%	46.6 ± 24.3%

pct. – percentile.
sd – standard deviation.
eBC – equivalent black carbon.
PNC – total particle number concentration (10 nm – 10 μm).
UFP – ultrafine particle number concentration (10 – 100 nm).
ACCU – accumulation mode particle number concentration (100 – 1000 nm).
COARSE – coarse mode particle number concentration (1000 nm – 10 μm).
ufp_nf – ultrafine particle number fraction.
accu_nf – accumulation mode particle number fraction.
PSAC – total particle surface area concentration.
UFP_SAC – ultrafine particle surface area concentration.
ACCU_SAC – accumulation mode particle surface area concentration.
COARSE_SAC - coarse mode particle surface area concentration.
ufp_saf – ultrafine particle surface area fraction.
accu_saf – accumulation mode particle surface area fraction.
TDSAC – Total respiratory tract deposited surface area concentration.
UFP_TDSAC – ultrafine particle respiratory tract deposited surface area concentration.
ACCU_TDSAC – accumulation mode particle respiratory tract deposited surface area concentration.
COARSE_TDSAC – coarse mode particle respiratory tract deposited surface area concentration.
ufp_dsaf – utrafine particle respiratory tract deposited surface area fraction.
accu_dsaf – accumulation mode particle respiratory tract deposited surface area fraction.
ADSAC – alveolar deposited total surface area concentration.
UFP_ADSAC – ultrafine particle alveolar deposited surface area concentration.
ACCU_ADSAC – accumulation mode particle alveolar deposited surface area concentration.
COARSE_ADSAC – coarse mode particle alveolar deposited surface area concentration.
ufp_adsaf – ultrafine particle alveolar deposited surface area fraction.
accu_adsaf – accumulation mode particle alveolar deposited surface area fraction.
ADSAD – Total alveolar deposited particle surface area dose.
UFP_ADSAD – ultrafine particle surface area dose deposited in alveolar region.
ACCU_ADSAD – accumulation mode particle surface area dose deposited in alveolar region.
COARSE_ADSAD – coarse mode particle surface area dose deposited in alveolar region.
ufp_adsadf – ultrafine particle surface area dose fraction deposited in alveolar region.
accu_adsadf – accumulation mode particle surface area dose fraction deposited in alveolar region.